Journal of
Nanoscience and Nanotechnology
Vol. 11, 10813–10816, 2011

Improved Charge Separation Properties of Organic Hetero-Junction Solar Cells by Self-Assembled Monolayers Anchored Ag Nanoparticles

Yian Tai*, Zong-Ci Guo, and Jadab Sharma†

Department of Chemical Engineering, National Taiwan University of Science and Technology, Taipei 106, Taiwan

We investigate the effect of self-assembled monolayers and localized surface plasmons of silver nano-particles on an organic solar cell consisting of zinc phthalocyanine as an active layer. The device was fabricated by covalent attachment of silver nanoparticles on *n*-type silicon substrates using self-assembled monolayer of 4-mercaptophenol. Power conversion efficiency is increased up to 8 times as compared to a reference device with merely 0.13% photo-conversion efficiency containing no self-assembled monolayers and silver nano-particles. We believe that improved conductivity at the interface due to the aromatic self-assembled monolayer and the increased local electric field experienced by the active layer in presence of silver nano-particles act in synergy towards the higher population of excitons and dissipation of charge.

Keywords: Solar Cell, Nanoparticles, Self-Assembled Monolayer, Localized Surface Plasmon Resonance.

1. INTRODUCTION

Improvement of photo-conversion properties at hetero-junctions between Si and metal free (H_2Pc) and metal substituted phthalocyanines (MPcs) may lead to construction of cost effective organic solar cells. PbPc, FePc, VoPc, MgPc, CuPc, and ZnPc are the organic *p*-type semiconductor materials that have been tested for photovoltaic applications.[1–7] Devices made from these materials with hetero-junctions, such as Ag/CuPc/p-Si, Au/p-MgPc/n-Si, and Au/ZnPc/Si have shown rectification and photoconversion properties with varied efficiencies.[6–8] However, the photoconversion efficiencies of such silicon based organic thin film cells are very low, partly due to the poor light absorptions and easy bulk and surface recombination of opposite charges. A drastic modification of the cell structure is needed to enhance the light absorption and to reduce the recombination process in order to increase their efficiencies. Recently, significant progresses have been made using surface plasmons of metal nanoparticles (NPs) due to their large optical cross sections as is demonstrated by both theoretical predictions and experiments.[9–11] The optical field enhancement due to the plasmons generation on nanoparticle surfaces can significantly enhance the power conversion efficiency as a result of increased exciton population, which in turn increases the light absorption ability of the nearby organic thin film.[12] However, exciton quenching at the NPs interfaces limits the potential efficiency gain. Apart from the limitations due to surface recombination, nature of hetero-junctions of photovoltaic devices plays the determining role for their electrical properties. It is highly essential, therefore, to understand the properties of such hetero-junctions at semiconductor interfaces, which could in essence help to improve the device outputs.

Indeed, a great deal of research effort has been devoted for the molecular level control over the energetics and kinetics of charge transfer processes across the semiconductor surfaces allowing manipulation of barrier heights of such systems.[13, 14] For example, chemical modification of Si(111) surfaces with short alkyl chains leads to the interfacial dipole moment change, while protecting the surface, it also creates rectifying junction.[15] Majority of such studies concern about avoiding Fermi-level pinning process associated with Schottky junctions. As a result, effort has been made to cast monolayer protected metal NP films on CH_3 terminated Si, which in turn generates unpinned Schottky junctions without interfacial reactivity.[16] Therefore, in principle and also in great extent practically, it is possible to control the electrical characteristics of conventional metal-semiconductor junctions with tunable barrier

*Author to whom correspondence should be addressed.
†Present address: CEMES/CNRS, UPR 8011, 29 rue Jeanne Marvig, 31055 Toulouse, France

1533-4880/2011/11/10813/004 doi:10.1166/jnn.2011.3995

heights simply by changing the functionality of the interlayer molecules.[17] In this work, however, we focus on the overall device characteristics of modified organic solar cells. We wish to investigate the combined effect of the localized surface plasmons of monolayer-protected silver NPs (Ag-NPs) and the electron transport properties of self-assembled monolayers (SAMs) on a ZnPc based organic solar cell (Au/ZnPc/Ag-NPs/SAM/Si/Al). Strong dependence of power conversion efficiency and short circuit current is observed on anchoring Ag-NPs to an aromatic SAM modified silicon substrate.

2. EXPERIMENTAL DETAILS

2.1. Reagents

4-mercaptophenol (MP, reagent grade) was obtained from Sigma Aldrich (USA) and used without further treatment. Oleic acid (reagent grade) and silver trifluroacetate (98%) were purchased from SHOWA Chemicals (Japan) and Acros Organics (USA), respectively. All organic solvents were of reagent grade and purchased either from Fischer Scientific (UK) or Acros Organics (USA). Deionized water used in different steps was obtained from a Milli Q reagent water system.

2.2. SAM Preparation

Si substrates used for fabrication of devices were treated with following successive steps.
(i) Substrates were refluxed in piranha solution (3 part H_2SO_4 and 1 part 30% v/v H_2O_2; caution: highly reactive) in a specially designed apparatus at 100 °C for 1 h followed by washing with copious amount of water. Substrates were then dried under flow of N_2.
(ii) Pretreated substrates were then immersed in 1:1 solution of NH_4OH and H_2O_2 for 15 min followed by washing and drying process as described in the Step 1.
(iii) Si substrates were again immersed in piranha solution at room temperature for 15 min and then washed thoroughly with water. After drying with N_2, Si substrates were stored for fabrication.

MP-SAM was formed by treating the substrate in a solution of 1 mM of 4-mercaptophenol in anhydrous toluene at 100 °C for 24 h. After the growth of SAM, substrate was immersed in ethyl acetate and cleaned in an ultrasonic bath for 1 min.

2.3. Synthesis of Ag-NPs

Silver trifluroacetate (0.04 g) was added to a flask containing isoamyl ether (5 mL) and magnetically stirred for 30 min under inert atmosphere (in a blanket of Ar).[18] Oleic acid (0.5 mL) was slowly added and stirring was continued for another 30 min. Temperature of the reaction mixture was then increased to 160 °C using an oil bath and refluxed at this temperature for 1 h under constant stirring. On cooling the reaction mixture to room temperature, 20 mL of ethanol was added followed by centrifugation at 5000 rpm for 20 min (the process was repeated for 3 times).

2.4. Organization of Ag NPs on Si-SAM Substrates

Silver nanoparticles were organized on Si-SAM substrates by covalent linking using ligand-exchange reaction.[19] A dispersion of Ag-NPs in hexane was used for the surface modification.

2.5. Device Fabrication

A standard deposition chamber with a precision film thickness controller unit was employed for the device fabrication.

2.6. Instrumentations

Current density–voltage (J–V) measurements were carried out under AM1.5 (100 mW/cm^2) illumination using a standard class A solar simulator (Oriel/Newport) and averaged for three independent measurements. UV-visible spectra were recorded with a JASCO V-670 Vis-NIR spectrophotometer. Transmission electron micrographs (TEM) images were acquired with a Philips Tecnai F30 Field-Emission-Gun Transmission Electron Microscope (FEG-TEM), equipped with EDAX attachment. Atomic force microscopic (AFM) images were obtained by tapping mode with a Veeco/DI NanoScope III, while external quantum efficiency (EQE) measurements were carried out with a Hamamatsu Photonics system. X-ray photoelectron (XP) spectrum was recorded by a VG-Thermo theta probe X-ray photoelectron spectrometer (XPS).

3. RESULTS AND DISCUSSION

Figure 1 gives the schematic description of a representative device consisting of an n-type silicon substrate modified with MP-SAM and Ag-NPs. We will describe devices made with different configurations as: '*device a*' for a device consisting of only ZnPc on a bare Si substrate, '*device b*' for a device consisting of ZnPc fabricated on a Si substrate that was pre-treated with Ag-NPs by a physical deposition method, and '*device c*' for a device consisting of a Si substrate with Ag-NPs anchored on MP-SAMs. In the succeeding discussions hereafter, we will compare our results considering the device '*a*' as the reference device, unless mentioned otherwise. All devices were fabricated by conventional thermal deposition of zinc phthalocyanine (ZnPc, 60 nm) thin layers on different Si substrates at room temperature, followed by the deposition of semitransparent Au thin layers (10 nm) with a designated effective area. While thin electrodes of Au and Al

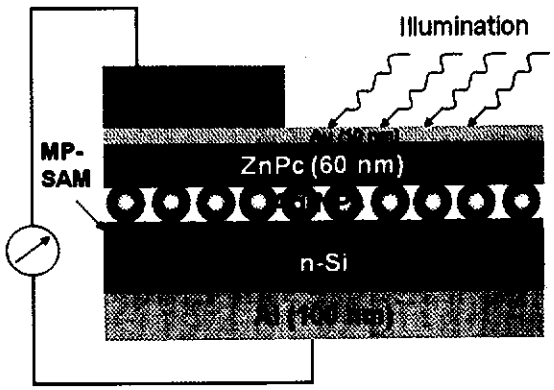

Fig. 1. Schematic description of the device '*c*' with the configuration of Si/MP-SAM/Ag-NPs/ZnPc.

(100 nm each) were deposited for top and bottom contacts, respectively.

Figure 2 shows (a) high resolution transmission electron micrograph of Ag-NPs, (b) XPS spectrum of 3d electrons of Ag-NPs anchored on a MP-SAM modified Si substrate, and (c) AFM image Ag-NPs anchored on MP-SAM. It is apparent from the TEM image that Ag-NPs are spherical in shape with nearly uniform size (average particle size: ~10 nm). The appearance of double peaks at 368.5 eV and 374.5 eV confirms the presence of metallic silver nanoparticles on the silicon surface. In particular, large number of Ag-NPs can be clearly seen from the AFM image of Ag-NPs anchored on a MP-SAM modified silicon substrate. It has been demonstrated recently that ideal distribution of nanoparticles on the surface is important for the optimized efficiency gain.[7]

Figure 3 shows the EQE spectra for devices '*a–c*'. The pronounce increment in EQE is a clear indication of the positive effect of localized surface plasmon resonance (SPR) of interlayer Ag-NPs for devices '*b*' and '*c*'. The

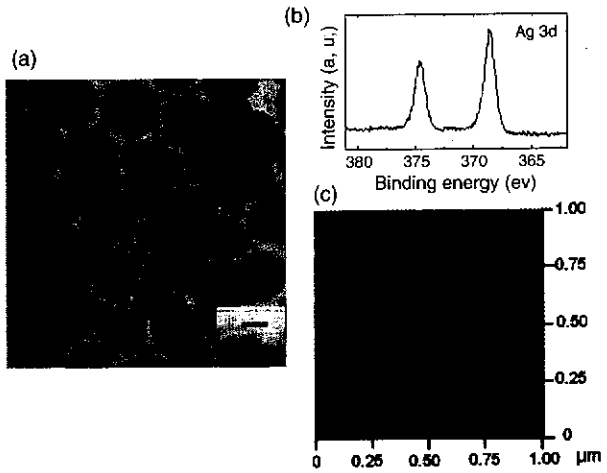

Fig. 2. (a) High resolution transmission electron micrograph of Ag-NPs, (b) XPS spectrum of 3d electrons of Ag-NPs anchored on a MP-SAM modified Si substrate, and (c) AFM image Ag-NPs anchored on MP-SAM.

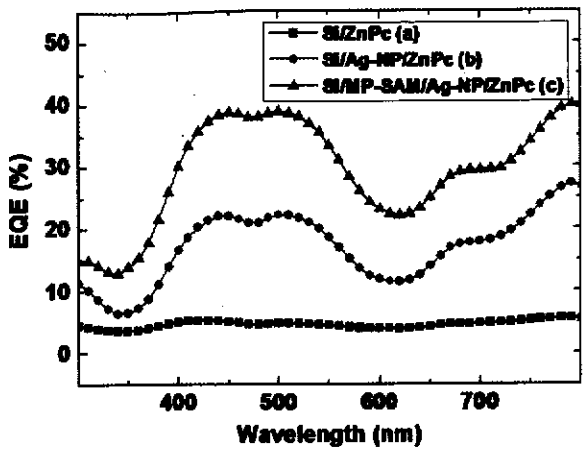

Fig. 3. External quantum efficiency (EQE) spectra for devices '*a–c*.'

maximum SPR effect was obtained for the device '*c*' when Ag-NPs were organized by covalent linkage to the aromatic SAM. The observed EQE for such a device is 35%, which is remarkably higher than the reference device with the value of less than 10%.

Evidently, SPR of Ag-NPs exerts a positive effect on the device which allows better absorption of light due to the enhanced electrical field experienced by the immediate active layer.[20,21] The SPR effect is the primary reinforcing factor in the external quantum efficiencies rather than due to the increased electron transport properties of aromatic SAMs on Si.[11] Notwithstanding to the dominating effect of SPR, SAM formation is a useful tool to modify the electronic properties of semiconductor surfaces.[22] As anticipated, EQE for the device '*b*' made by sandwiching a layer of NPs between Si and ZnPc gives a better EQE value (~25%) as compared to the reference device with no nanoparticles. The above results suggested that SPR effect and enhanced electron transport, both act in synergy for the device '*c*' showing increased exciton population and facile dissipation of charge through the aromatic SAM.[10,21,23]

A comparative study on electrical properties of devices '*a–c*' helped us to understand the effect of plasmons on the generation of excitons and dissipation of charge. Device '*c*' shows a high value of open circuit potential (V_{oc}, 0.44 V) which also produces a significantly higher short-circuit photocurrent density (J_{sc}) of 10.4 mAcm^{-2}. A close correlation between the results of electrical measurements, a summary of which is given in Table I, and EQE experiments is observed. Although, J_{sc} of device '*b*' is improved, V_{oc} is still smaller than the reference device. Clearly, two emerging crucial factors which determine the device properties are (i) how Ag-NPs were organized and (ii) nature of the interface. Presumably, the SPR contributions on device efficiency easily override the large gain associated with the facile electron transport properties of aromatic SAM.[23–25] Reasonably, device '*c*' with all positive enhancement effects resulted from the covalent linkage and

Table I. Device parameters for solar cells '*a–c*' with the configurations of Si/ZnPc, Si/Ag-NPs/ZnPc, and Si/MP-SAM/Ag-NPs/ZnPc, respectively.

Device	J_{sc} (mA/cm^2)	η(%)	V_{oc} (mV)
(a) Si/ZnPc	1.4	0.13	420
(b) Si/Ag-NPs/ZnPc	5.07	0.33	340
(c) Si/MP-SAM/Ag-NPs/ZnPc	10.4	1.15	440

facile electron transport though aromatic SAM shows the maximum efficiency (1.15%) and J_{sc} (10.4 mA cm^{-2}).

The reason for the drastically different behaviors of different devices (*a–c*) is that the work function barrier between Si substrate and active layer is high which implies that electron transport at the interface is partially blocked. This blocking effect is effectively minimized by introducing a layer of Ag-NPs which reduces the barrier as well as alters the local electrical field associated with the active layer, in turn greatly enhancing the light absorption properties.[26] This blocking effect is effectively circumvented for the device '*c*' with an aromatic SAM, where electron transport is increased due to the improved carrier tunneling or conductance properties of aromatic SAM (reduced barrier effect).[27,28] This is manifested by marginal increase of the V_{oc}. Indeed, charge carrier tunneling is the deciding factor for other devices as well, such as pseudo metal-oxide-semiconductor field-effect transistors (MOSFET), where modulation of electrical properties has been accomplished by the monolayers of grafted π-acceptor or π-donor molecules atop silicon surfaces.[23] Since, EQE is defined as the ratio of collected charges to incident photons, effective charge carrier through the acceptor is important for the device efficiency. Thus, the factor which influences the short-circuit current also controls the efficiency. The importance of charge dissipation and the dependency of local exciton generation on specific geometries in bilayer organic solar cells has been explained recently.[29]

4. CONCLUSIONS

In summary, we have demonstrated the effect of monolayer properties and localized surface plasmons of silver nanoparticles on an organic photovoltaic device. Device efficiency is improved significantly on incorporation of Ag-NPs anchored on an aromatic SAM. A synergetic effect is observed as a result of enhanced light absorption due to the surface plasmons of silver nanoparticles and easy charge dissipation through the aromatic SAM.

Acknowledgments: The authors thank Chien-Hung Lin, Yuan-Kui Liu and Shao-Chin Tseng for useful discussions at various levels. This work was supported by Academia Sinica (nano-2394) and National Science Council (96-2113-M-011-002-MY2).

References and Notes

1. C. W. Tang, *Appl. Phys. Lett.* 48, 183 (**1986**).
2. Y. Terao, H. Sasabe, and C. Adachi, *Appl. Phys. Lett.* 90, 103515 (**2007**).
3. A. Ahmed and R. A. Collins, *Phys. Stat. Sol. (A)* 123, 201 (**1991**).
4. H. S. Soliman, M. M. El-Nahass, A. M. Farid, A. A. M. Farag, and A. A. El-shazly, *Eur. Phys. J. Appl. Phys.* 21, 187 (**2003**).
5. S. Riad, *Thin Solid Films* 370, 253 (**2003**).
6. B. Remaki, G. Guillaud, and D. Mayes, *Opt. Mater.* 9, 240 (**1998**).
7. A. M. Saleh, A. K. Hassan, and R. D. Gould, *J. Phys. Chem. Solids* 64, 1297 (**2003**).
8. S. Antohe, N. Tomozeiu, and S. Gogonea, *Phys. Stat. Sol. (A)* 125, 397 (**1991**).
9. J. R. Cole and N. J. Halas, *Appl. Phys. Lett.* 89, 153120 (**2006**).
10. J. Hagen, W. Schaffrath, P. Otschik, R. Fink, A. Bacher, H.-W. Schmidt, and D. Haarer, *Synthetic Metals* 89, 215 (**1997**).
11. B.-H. Kim, C.-H. Cho, J.-S. Mun, M.-K. Kwon, T.-Y. Park, J. S. Kim, C. C. Byeon, J. Lee, and S.-J. Park, *Adv. Mater.* 20, 3100 (**2008**).
12. K. R. Catchpole and S. Pillai, *J. Lumnescence* 121, 315 (**2006**).
13. R. Cohen, N. Zenou, D. Cahen, and S. Yitzchaik, *Chem. Phys. Lett.* 279, 270 (**1997**).
14. R. Hunger, R. Fritsche, B. Jäckel, L. J. Webb, W. Jaegermann, and N. S.Lewis, *Surf. Sci.* 601, 2896 (**2007**).
15. S. Maldonado, K. E. Plass, D. Knapp, and N. L. Lewis, *J. Phys. Chem. C* 111, 17690 (**2007**).
16. S. Maldonado, D. Knapp, and N. L. Lewis, *J. Am. Chem. Soc.* 130, 3300 (**2008**).
17. A. Vilan, A. Shanzer, and D. Cahen, *Nature* 404, 166 (**2000**).
18. X. Z. Lin, X. Teng, and H. Yang, *Langmuir* 19, 10081 (**2003**).
19. Y. Song and R. W. Murray, *J. Am. Chem. Soc.* 124, 7096 (**2002**).
20. B. P. Rand, P. Peumans, and S. R. Forrest, *J. Appl. Phys.* 96, 7519 (**2004**).
21. C. Hägglund, M. Zäch, and B. Kasemo, *Appl. Phys. Lett.* 92, 013113 (**2008**).
22. H.-Z. Yu, S. Morin, D. D. M. Wayner, P. Allongue, and C. H. de Villeneuve, *J. Phys. Chem. B* 104, 11157 (**2000**).
23. T. He, J. He, M. Lu, H. Pang, W. F. Reus, W. M. Nolte, D. P. Nackashi, P. D. Franzon, and J. M. Tour, *J. Am. Chem. Soc.* 128, 14537 (**2006**).
24. K. Kim and D. L. Carroll, *Appl. Phys. Lett.* 87, 203113 (**2005**).
25. A. J. Morfa, K. L. Rowlen, T. H. Reilly, III, M. J. Romero, and J. van de Lagemaat, *Appl. Phys. Lett.* 92, 013504 (**2008**).
26. M. Schnippering, M. Carrara, A. Foelske, R. Kötz, and D. J. Fermin, *Phys. Chem. Chem. Phys.* 9, 725 (**2006**).
27. C. Boulas, J. V. Davidovits, F. Rondelez, and D. Vuillaume, *Phys. Rev. Letts.* 76, 4797 (**1996**).
28. H. B. Akkerman and B. de Boer, *J. Phys. Condens. Matter.* 20, 013001 (**2008**).
29. Ch. Breyer, M. Vogel, M. ohr, B. Johnev, and K. Fostiropoulos, *Phys. Stat. Sol. B* 243, 3176 (**2006**).

Received: 30 December 2009. Revised/Accepted: 30 August 2010.

RESEARCH ARTICLE